

# Scattering of Magnetic Solitons in two dimensions

S. Komineas

*Physikalisches Institut, Universität Bayreuth, D-95440 Bayreuth, Germany  
e-mail: stavros.komineas@uni-bayreuth.de*

Solitons which have the form of a vortex-antivortex pair have recently been found in the Landau-Lifshitz equation which is the standard model for the ferromagnet. We simulate numerically head-on collisions of two vortex-antivortex pairs and observe a right angle scattering pattern. We offer a resolution of this nontrivial dynamical behaviour by examining the Hamiltonian structure of the model, specifically the linear momentum of the two solitons. We further investigate the dynamics of vortices in a modified nonlinear  $\sigma$ -model which arises in the description of antiferromagnets. We confirm numerically that a robust feature of the dynamics is the right angle scattering of two vortices which collide head-on. A generalization of our theory is given for this model which offers arguments towards an understanding of the observed dynamical behaviour.

## I. INTRODUCTION

Localized solutions, often called solitons, play an increasingly important role in nonlinear field theories in two dimensions. Topological structures exist in particular in magnetic systems and have been studied extensively, both theoretically and experimentally [1,2].

An easy-plane ferromagnet is described by the Landau-Lifshitz equation

$$\dot{\mathbf{n}} = \mathbf{n} \times \mathbf{f}, \quad (1)$$

$$\mathbf{f} = \Delta \mathbf{n} - n_3 \hat{\mathbf{e}}, \quad \mathbf{n}^2 = 1.$$

The field  $\mathbf{n}$  represents the local magnetization of the material. We shall study here the case of a two-dimensional medium so we assume  $\mathbf{n} = \mathbf{n}(x, y, t)$ . The dot denotes a time derivative,  $n_3$  is the third component of  $\mathbf{n}$ ,  $\Delta$  is the Laplace operator and  $\hat{\mathbf{e}} = (0, 0, 1)$  is the unit vector in the third direction. The normalization condition  $\mathbf{n} = 1$  imposed in the initial condition is preserved by the equations of motion.

Static solutions of model (1) are the well-studied vortices. Isolated vortices are spontaneously pinned objects that is no vortex in free translational motion can be found in a 2D ferromagnet. The same is true for any isolated object with nontrivial topology in a 2D ferromagnet [3], the most well-known example being the magnetic bubbles in easy-axis ferromagnetic films [1].

Coherently traveling solutions of (1) have been found in [4]. They have the form of a vortex-antivortex pair and their velocity may take any value between zero and unity, which is the velocity of magnons in the system.

We now turn to a different class of systems, namely antiferromagnets. The dynamics of the staggered magnetization in the antiferromagnetic continuum is given by the nonlinear  $\sigma$ -model [2,5,6]:

$$\mathbf{n} \times [\ddot{\mathbf{n}} - \mathbf{f}] = 0, \quad (2)$$

$$\mathbf{f} = \Delta \mathbf{n} - n_3 \hat{\mathbf{e}}, \quad \mathbf{n}^2 = 1,$$

where the double dot denotes a second time derivative. The above model has the same static vortex solutions as (1). On the other hand, vortices in model (2) can be found in free translational motion. This is due to the fact that the model is invariant under Lorentz transformations.

Our main purpose is to study collisions of solitons in models (1) and (2). In the ferromagnet no collision between two vortices can take place. Two vortices with the same topological charge will rotate around each other while a vortex and an antivortex undergo Kelvin motion perpendicular to the line connecting them. However, collisions can occur between two vortex-antivortex pairs. We elaborate on the arguments of [4,7] and argue that head-on collisions between vortex-antivortex pair solitons give a right angle scattering pattern.

We also study collisions between vortices in antiferromagnets in Eq. (2). They scatter at right angles as found in numerical simulations. In fact, the right angle scattering phenomenon seems to be a robust feature in various two-dimensional models which have soliton solutions [8,9]. However, it is a nontrivial and strange behaviour at least from the point of view of scattering of ordinary particles.

The colliding objects in the two models that we study are essentially different from each other. While vortices within model (2) are topologically nontrivial objects, the colliding vortex-antivortex pairs in (1) have a vanishing topological charge. However, we argue that the underlying Hamiltonian structure allows to study the soliton interaction in the two models in close analogy.

The outline of the paper is as follows. In Section II we simulate head-on collisions of vortex-antivortex pairs in (1) and give a theoretical description which exploits the form of the linear momentum. In Section III the results of head-on collision simulations of vortices in model (2) are given together with arguments for the understanding of this behaviour. The conclusions are given in Section IV.

## II. HEAD-ON COLLISIONS OF VORTEX-ANTIVORTEX PAIRS IN PLANAR FERROMAGNETS

A ferromagnet can be described in terms of a magnetization vector which satisfies the Landau-Lifshitz equation (1). The constraint on the field  $\mathbf{n}$  can be resolved and the theory can be formulated in terms of a complex variable

$$\Omega = \Omega(x, y, t) = \frac{n_1 + i n_2}{1 + n_3} \quad (3)$$

which satisfies the equation

$$i \dot{\Omega} = -\Delta \Omega + \frac{2\bar{\Omega}}{1 + \Omega\bar{\Omega}} \partial_\mu \Omega \partial_\mu \Omega - \frac{1 - \Omega\bar{\Omega}}{1 + \Omega\bar{\Omega}} \Omega. \quad (4)$$

$\bar{\Omega}$  denotes the complex conjugate of  $\Omega$ .

We use the formulation through the complex variable  $\Omega$  in all numerical simulations. We avoid the formulation through the vector variable  $\mathbf{n}$  since the constraint on it makes an accurate computer calculation of the time derivatives of the field rather cumbersome.

The model has some interesting static vortex solutions of the form

$$\Omega^\circ = f(\rho) e^{i\kappa\phi}, \quad \kappa = \pm 1, \quad (5)$$

where  $\rho, \phi$  are polar coordinates and  $f(\rho = 0) = 0, f(\rho \rightarrow \infty) \rightarrow 1$ . We call the configuration with  $\kappa = 1$  a vortex and the one with  $\kappa = -1$  an antivortex. Vortex solutions have infinite energy and it has been argued that they are physically relevant [10,6].

In the study of the dynamics of magnetic vortices the central role is played by a scalar quantity called the local vorticity [3,6]

$$\gamma = \varepsilon_{\mu\nu} \partial_\mu \pi \partial_\nu \psi, \quad (6)$$

where  $\varepsilon_{\mu\nu}$  is the two-dimensional totally antisymmetric tensor. The two components of the linear momentum are then expressed as

$$p_x = - \int y \gamma \, dx dy, \quad p_y = \int x \gamma \, dx dy. \quad (7)$$

Of fundamental importance is the Poisson bracket relation between the two components of the linear momentum. This reads

$$\{p_x, p_y\} = \Gamma, \quad (8)$$

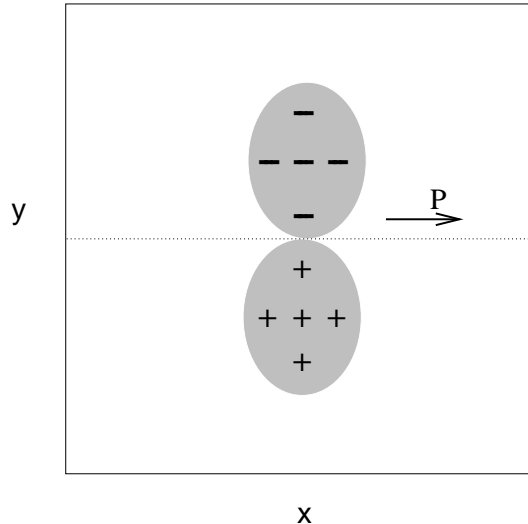


FIG. 1. A simple vorticity distribution of a soliton consists of two lumps with opposite sign. They are here symmetrically placed on either side of the  $x$ -axis. The lower shaded area represents positive vorticity while the upper shaded area represents negative vorticity.  $P$  denotes the linear momentum of the pair.

where

$$\Gamma = \int \gamma \, dx dy \quad (9)$$

is the total vorticity.

In the present model  $\pi = \cos\Theta$  and  $\psi = \Phi$  have been used [3] as the canonical fields. They are defined through  $n_1 = \cos\Theta \sin\Phi, n_2 = \sin\Theta \sin\Phi, n_3 = \cos\Theta$ . The explicit form of the vorticity is

$$\gamma = \varepsilon_{\mu\nu} \sin\Theta \partial_\nu \Theta \partial_\mu \Phi. \quad (10)$$

The total vorticity of a vortex is

$$\Gamma = \int \gamma \, dx dy = -2\pi\kappa, \quad (11)$$

that is,  $\Gamma = -2\pi$  for vortices and  $\Gamma = 2\pi$  for antivortices.

The implications of a nonvanishing total vorticity to the dynamics is an issue which has been thoroughly studied in the case of magnetic vortices and bubbles [3,6,11] as well as in the case of vortices in other interesting models [12,13]. The most striking result is that it leads to spontaneous pinning of these topological objects.

Since a nonvanishing total vorticity  $\Gamma$  implies pinning of an object, we infer that a solution which moves freely should have a vanishing  $\Gamma$ . In this respect, the vortex-antivortex ansatz offers the simplest possibility. Fig. 1 gives a schematic representation of it. This consists of two lumps, one having negative and the other one positive sign. We suppose that the vortex is roughly laying in the shaded area with the negative sign and the antivortex in the shaded area with the positive sign. This figure

is supposed to act only as a guide for our discussion and there is no strict way to distinguish the two vortices and define their positions. However, if relation (8) is applied to each vortex separately then the quantity on the right hand side is nonvanishing. It is then implied that each vortex will propagate in the horizontal direction under the influence of the other vortex. The picture is consistent with linear momentum considerations. That is, an application of Eq. (7) to the full ansatz gives a nonvanishing  $x$ -component of the linear momentum. Fig. 1 will serve in the following discussion as a prototype and will motivate our theoretical arguments.

The Kelvin motion of a vortex-antivortex pair in a ferromagnet has been investigated in [14]. The motion of a bubble-antibubble ansatz has also been studied [15]. The situation is found to be similar in some other systems such as an antiferromagnet immersed in a uniform magnetic field [6], a model for superconductors [16], for superfluid helium [17] and the nonlinear Schrödinger equation [18]. It has been pointed out that the gross features of this dynamical behaviour are analogous to the planar motion of charges under the influence of a magnetic field perpendicular to the plane. In particular, two oppositely charged particles undergo Kelvin motion traveling along parallel trajectories. The analogy has been made precise by use of relation (8) and an analogous relation in the charge motion problem [3].

The calculation of steadily moving coherent structures in a 2D ferromagnet, which have the form of a vortex-antivortex pair has been done in [4]. We have used here the numerical code of [4] to reproduce them since there is no available analytical formula. Fig. 2 is an example contour plot for a soliton with velocity  $v=0.5$ . The upper entry gives contour plots of the quantity  $10|\Omega|$  and the two-vortex character of the configuration is rather obvious. The lower entry is a contour plot for the local vorticity (10). An important result of the analysis in [4] is that the velocity is collinear with the linear momentum.

We are now sufficiently motivated to explore the possibility of scattering of vortex-antivortex pair solitons. We denote by  $\Lambda_v(x, y)$  the solution with velocity  $v$  along the  $x$ -axis (set  $t=0$ ). The product ansatz

$$\Omega(x, y) = \Lambda_v\left(x + \frac{\delta}{2}, y\right) \Lambda_{-v}\left(x - \frac{\delta}{2}, y\right) \quad (12)$$

represents two vortex-antivortex pair solitons at a distance  $\delta$  apart which are in a head-on collision course. The ansatz (12) is used as an initial condition in a straightforward numerical integration of Eq. (4). We typically set  $v=0.5$ ,  $\delta=10$ .

We have set up a numerical mesh as large as  $600 \times 600$  with uniform lattice spacing  $h=0.1$ . The space derivatives are calculated by finite differences and the time integration is performed by a fourth order Runge-Kutta method. The results are presented in Figs. 3 and 4. Fig. 3 presents a contour plot for the field  $10|\Omega|$  at three characteristic snapshots. In the first entry the initial ansatz

(12) is shown. The second snapshot is taken when the solitons are more or less at a minimum separation. No vortex-antivortex annihilation process takes place. This behaviour should be expected since the vortex-antivortex pair solitons are stable solutions of the equation. The argument is supported by numerical simulations showing that a vortex-antivortex ansatz preserves its character when traveling, provided that the vortex and antivortex are not very close to each other [14,6]. The last snapshot shows the system after the collision. A right angle scattering pattern has been produced.

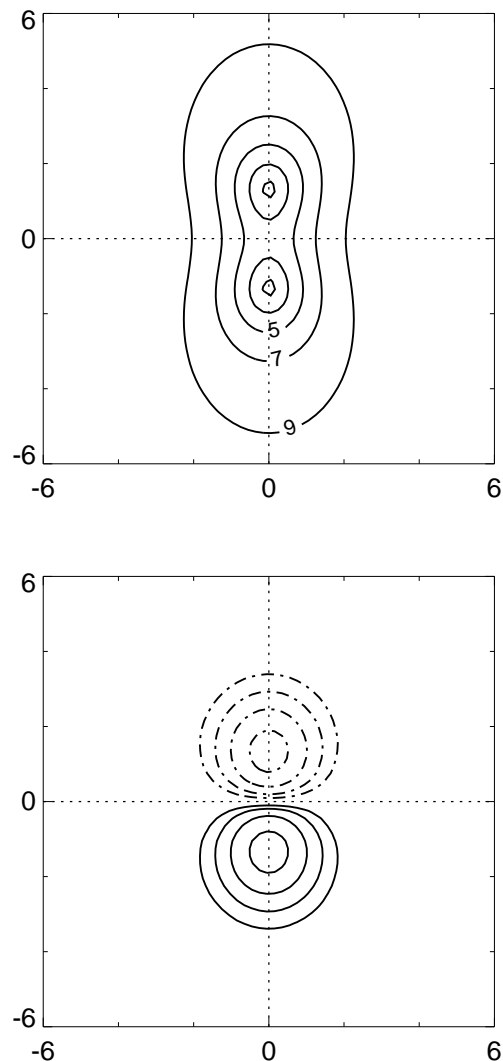


FIG. 2. Contour plot for a vortex-antivortex pair soliton in a ferromagnet with velocity  $v=0.5$ . The upper entry gives contour plots of the quantity  $10|\Omega|$ . We plot the levels 1, 3, 5, 7, 9. The lower entry is a contour plot of the local vorticity for the same soliton. Solid lines represent positive values and dashed-dotted lines negative values of vorticity. We plot the levels  $\pm 0.1, \pm 0.2, \pm 0.4, \pm 0.8, \pm 1.2$ .

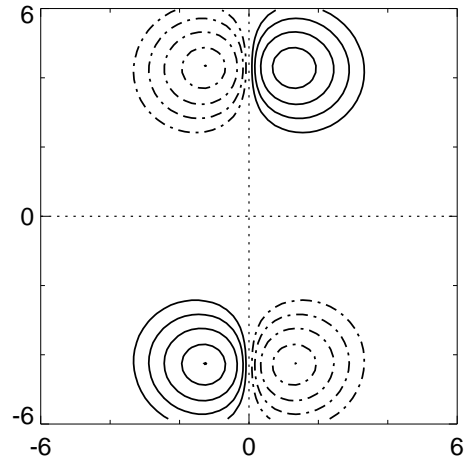
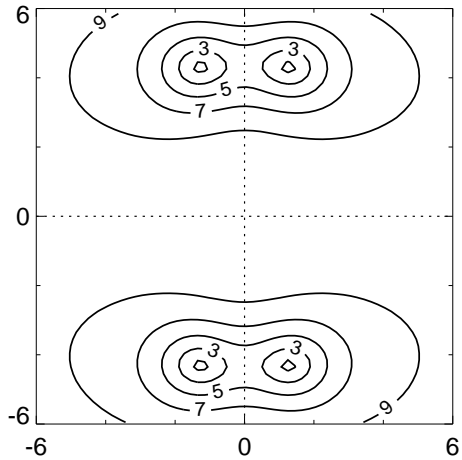
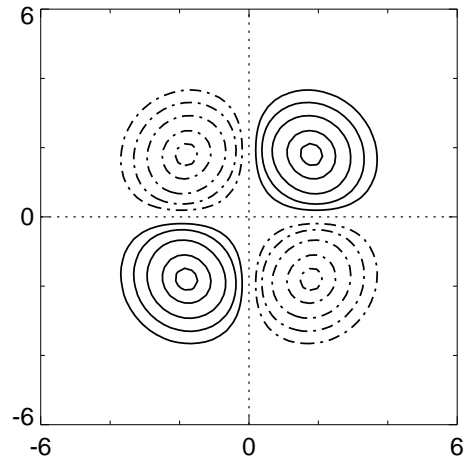
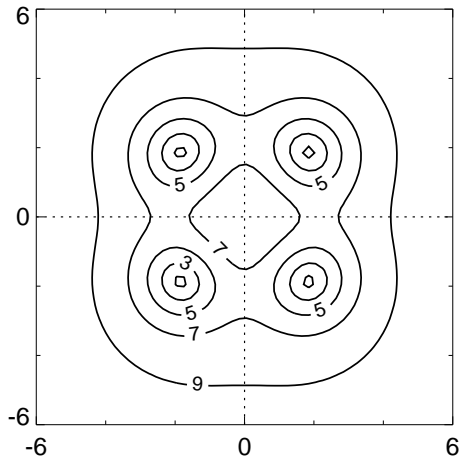
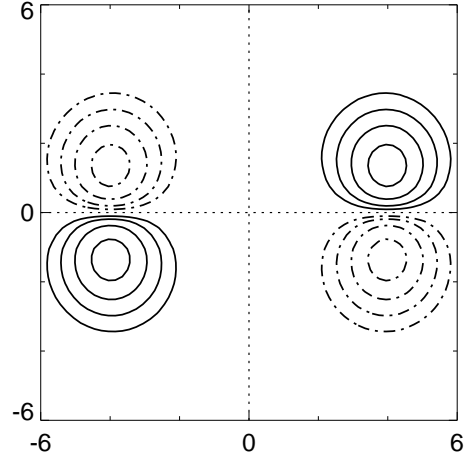
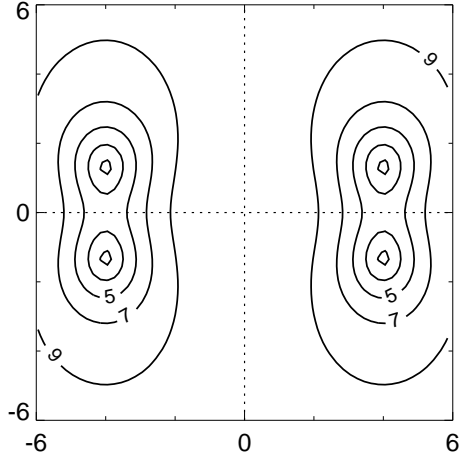


FIG. 3. Contour plot of the field  $10|\Omega|$  at three characteristic snapshots of the head-on collision simulation of vortex-antivortex pair solitons in ferromagnets. It is shown: the initial ansatz (upper entry, time  $t=0$ ), a snapshot at the time of collision (middle entry,  $t=6.6$ ), and well after collision (lower entry,  $t=13.2$ ). Contour levels as in Fig. 2.

FIG. 4. Contour plot of the local vorticity  $\gamma$  of Eq. (10) for the solitons of Fig. 3. Contour levels as in Fig. 2.

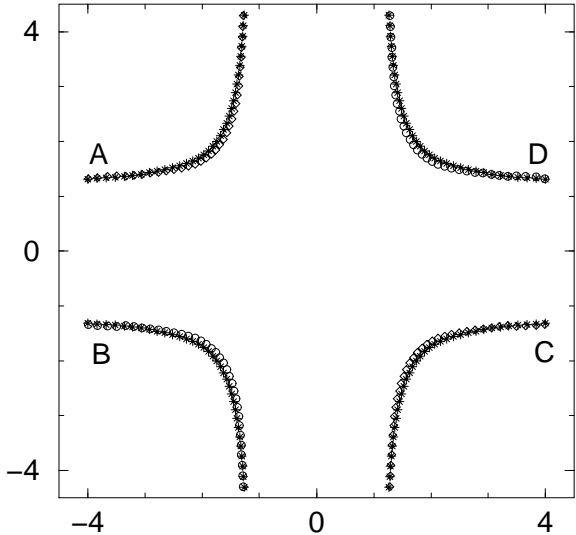


FIG. 5. Stars denote the zeros of  $\Omega$  during the numerical simulation of Fig. 3. We also trace the maximums (circles) and minimums (diamonds) of the vorticity. The solitons are initially located at  $AB$  and  $CD$  respectively. Symbols are plotted every 0.4 time units.

The situation becomes clearer in Fig 4 where we represent the solitons in terms of their local vorticity distribution. The soliton on the left half plane should be compared directly with that in the lower entry of Fig. 2. It obviously has a linear momentum and velocity pointing to the positive  $x$ -direction. The other soliton has the opposite linear momentum and velocity.

It is rather clear from the picture that the solitons will not bounce back after collision. This is precluded by the form of the local vorticity distribution. This possibility would require that the vortex and antivortex interchange their position. Instead, the possibility appears that, at collision time, the two pairs of vorticity lumps in the upper and lower half-planes will form two new vortex-antivortex pairs.

One has to apply Eq. (8) for each of the vorticity lumps separately. Alternatively, one can consider pairs of lumps which tend to travel parallel to each other undergoing Kelvin motion. Application of this idea to Fig. 4, determine the time evolution of the system. Finally, the two pairs on the upper and lower half planes tend to travel parallel to each other along the  $y$ -axis and form bound states.

An equivalent point of view is to follow the linear momentum of each soliton separately. The linear momentums of the outgoing solitons clearly lay on the  $y$ -axis and have opposite sign.

A subtle but important question is whether we can apply Eq. (8) separately for each of the vortices which consist the vortex-antivortex pair. A rigorous answer can not be given here. On the other hand the construction of solitary waves in [4,7,17] suggests an affirmative answer

whose range of validity is interesting to study.

The two solitons emerging after collision are very similar to the initial ones though not exactly the same. In fact the drift velocity of the outgoing solitons is somewhat larger. In Fig. 5 we have traced, during the time evolution, the points where the complex field  $\Omega$  vanishes and also the points where the vorticity  $\gamma$  attains its maximum and minimum values. The two kinds of extrema are close during the whole period of time evolution. This is because the solitons used in the simulations of this chapter have a pronounced vortex-antivortex character. In [19] traveling solutions of the Landau-Lifshitz equation have been studied which are different than the ones used here. Numerical simulations of scattering of these solitons also produce a right angle pattern.

It is possible to give a picture, corresponding to the scattering of vortex-antivortex pairs, in terms of 2D motion of charged particles interacting via their electric field and placed in a magnetic field perpendicular to the plane. In fact, we have to consider two electron-positron pairs. Consider the first electron-positron pair located at points  $A, B$  of Fig. 5. and the second pair at  $C, D$ . The charges move similar to the vortices. Their actual orbits resemble those for the solitons shown in Fig. 5.

Our last remark in this section goes to some related work in hydrodynamics. There are solutions of the two-dimensional Euler equations which describe vorticity dipoles. Note that, in this context, vorticity has its ordinary hydrodynamic meaning. The best-known such solution seems to be the Lamb dipole [20]. Another one has been found in [21]. A head-on collision between two dipoles produces a pattern analogous to that in Fig. 4 of the present paper [21,22]. Furthermore, a simple construction is given in [20] page 223, to which our Fig. 5 can be compared. Further interesting cases of scattering between pairs of objects in hydrodynamics have been studied. The most complex behaviour has been observed in [23] and includes stochastic and quasiperiodic motion of vortices.

### III. HEAD-ON COLLISIONS OF VORTICES IN ANTIFERROMAGNETS

Our main objective is to study scattering of vortices within model (2) and to show that the process can be studied in close analogy to the corresponding phenomenon in the ferromagnet. A right angle scattering behaviour of solitons has been observed in the isotropic  $\sigma$ -model [8], that is model (2) without the anisotropy term.

The examination of the local vorticity  $\gamma$  has led to a successful approach for the collision of vortex-antivortex pairs in ferromagnets in Section II. We find it instructive to look at the collision process in terms of the vorticity also in the present model. A simple generalization of definition (6) can be used [6]. The vorticity attains a simple form when it is expressed in terms of the vector field  $\mathbf{n}$ :

$$\gamma = \varepsilon_{\mu\nu} \partial_\mu \dot{\mathbf{n}} \cdot \partial_\nu \mathbf{n} = \varepsilon_{\mu\nu} \partial_\mu (\dot{\mathbf{n}} \cdot \partial_\nu \mathbf{n}). \quad (13)$$

In [6] the equation for an antiferromagnet in a uniform magnetic field was studied. Vortices in this system are spontaneously pinned, thus their dynamics is analogous to that of ferromagnetic vortices. This unexpected behaviour is probed by a topological term which enters the vorticity. However, such a term is absent in the model studied in this section.

The vorticity (13) has the form of a total divergence and can be integrated in all space to show that the total vorticity vanishes for solutions with reasonable behaviour at infinity:

$$\Gamma = \int \gamma \, dx dy = 0. \quad (14)$$

In particular, it vanishes for the vortex solutions. Relations (7) - (9) apply in the present context without modification and they will be the fundamental relations to be used in the following analysis.

Eq. (13) shows that for a static vortex  $\gamma$  vanishes identically. On the other hand, we can obtain a steadily traveling vortex by applying a Lorentz transformation to the static vortex solution (5). We denote the traveling vortex by  $\Omega_v^\circ$  and the velocity is  $0 < v < 1$ . The distribution of  $\gamma$  for a Lorentz boosted vortex is nonvanishing and can be calculated numerically. The vortex with velocity  $v=0.7$  is represented by a contour plot of the field  $10|\Omega|$  in the upper entry of Fig. 6. A corresponding plot for  $\gamma$  is given in the lower entry of the figure.

The vorticity distribution has the form of two lumps, thus it resembles the sketch of Fig. 1. This is no surprise. In fact the following two remarks make it plausible. Firstly, we see that the total vorticity vanishes according to relation (14). Secondly, an inspection of the form (7) of the linear momentum makes it clear that a nonvanishing component is furnished by two lumps of vorticity with opposite signs. This is not the only form of local vorticity that furnishes a nonvanishing linear momentum but it is certainly the simplest. Since the vortex solution with  $\kappa=1$  is indeed the one with the simplest topological complexity, we expect its vorticity distribution to have the simplest possible form.

We calculate numerically the points where the maximum and minimum of the vorticity lumps are located. It turns out that these points are the  $(0, \pm 0.59)$  for any value of the velocity  $v$ .

A further example on the present ideas is offered by the Belavin-Polyakov solutions [24]. We apply a Lorentz transformation, with velocity  $v$ , to the simplest one:  $\Omega = (x - vt)/\sqrt{1 - v^2} + iy$ . Its local vorticity is

$$\gamma = -\frac{16v}{1 - v^2} \frac{y}{\left(1 + \frac{(x-vt)^2}{1-v^2} + y^2\right)^3}. \quad (15)$$

In accordance with the above remarks, it has the shape of two lumps with opposite sign, located on either side of the  $x$ -axis and traveling along the  $x$ -axis.

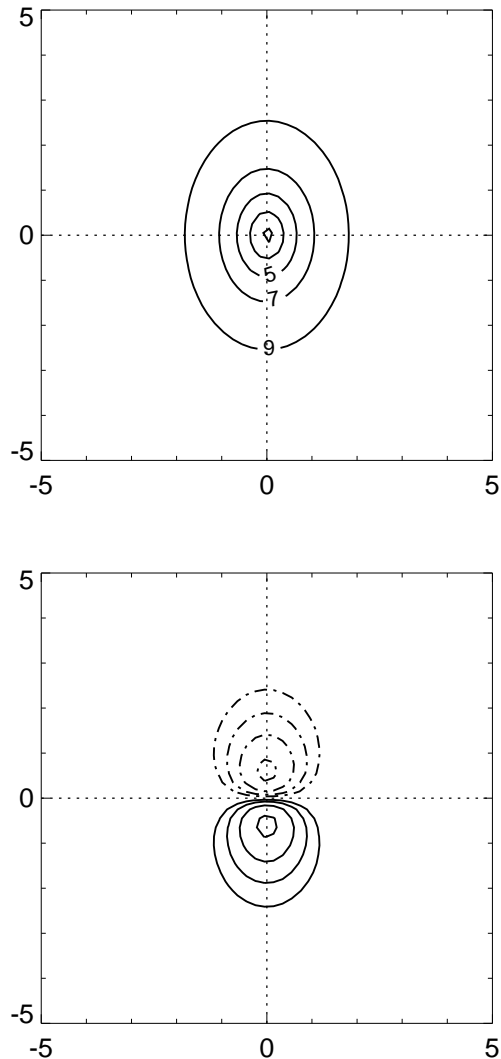


FIG. 6. Contour plot for a traveling vortex with velocity  $v = 0.7$ . The upper entry gives contours of the field  $10|\Omega|$ . The lower entry is a contour plot of the local vorticity  $\gamma$ . Solid lines represent positive values and dashed-dotted lines represent negative values of vorticity. Contour levels as in Fig. 2.

We are now ready to present numerical simulations of head-on collisions of vortices. We make an ansatz representing two vortices. The choice is not unique and the simplest one seems to be the product ansatz:

$$\Omega(x, y) = \Omega^\circ \left( x + \frac{\delta}{2}, y \right) \Omega^\circ \left( x - \frac{\delta}{2}, y \right), \quad (16)$$

where  $\Omega^\circ$  is the single vortex solution given in Eq. (5). The two vortices are a distance  $\delta$  apart.

The numerical mesh as well as the details of the algorithm that we use here are similar to those of Section II. We use vortices with  $\kappa=1$ . They are initially at rest but

immediately start to drift away from each other due to their mutual repulsion and escape to infinity.

In order to invoke a head-on collision between vortices we consider the product ansatz of two vortices which have opposite velocities:

$$\Omega(x, y) = \Omega_v^o \left( x + \frac{\delta}{2}, y \right) \Omega_{-v}^o \left( x - \frac{\delta}{2}, y \right). \quad (17)$$

$\Omega_v^o(x, y)$  denotes the Lorentz transformed vortex solution with velocity  $v$ , at  $t=0$ .

We typically use  $\delta=6$ . In all simulations the vortices start to move against each other with velocities close to the value  $v$  but they immediately begin to decelerate due to their mutual repulsion. The future of the process depends crucially on the magnitude of the velocity. At low velocities the two vortices approach to a minimum distance at which they come to rest and then turn round and move off in opposite directions. When the velocity exceeds a critical value (which is  $v_c \approx 0.65$  for  $\delta=6$ ) the two vortices collide and scatter at right angles. This result does not depend on the details of the initial ansatz or on the initial velocity of the vortices, as long as this exceeds the critical value. We have tested our algorithm for velocities up to the value  $v=0.9$  in ansatz (17). However, one must keep in mind that the velocity of the vortices at the time of collision is smaller than the velocity in the initial ansatz.

In Fig. 7 we give a contour plot for the norm of the field  $\Omega$  at three characteristic snapshots. The first entry presents the initial configuration (17). In the middle snapshot, taken at collision time, it is clear that the two vortices come on top of each other. There is no topological reason, related to the field  $\Omega$ , that could prevent this double vortex to form and there is also no such reason that could prevent the vortices either to continue traveling in the horizontal direction or to reemerge traveling in the vertical direction. We add that, at the present level of description, we can find no reason that would enforce them to follow either of the two possibilities. In the last snapshot the two new vortices that emerge after the collision, are drifting away from each other along the  $y$ -axis.

We find it instructive to look at the collision process using the vorticity. Our description will closely follow that in Section II in connection with the scattering of vortex-antivortex pairs. The dynamics in both systems is determined by the corresponding vorticity distribution. A comparison of the lower entries of Figs. 2 and 6 gives a hint that the underlying dynamics should be of a similar nature in both models.

In Fig. 8 we give the vorticity at three snapshots which correspond to those of Fig. 7. Fig. 8 should be compared directly with Fig. 4. An examination of these results shows that the arguments of Section II for the soliton scattering which rely upon the linear momentum relations (7), (8) are applicable here, too.

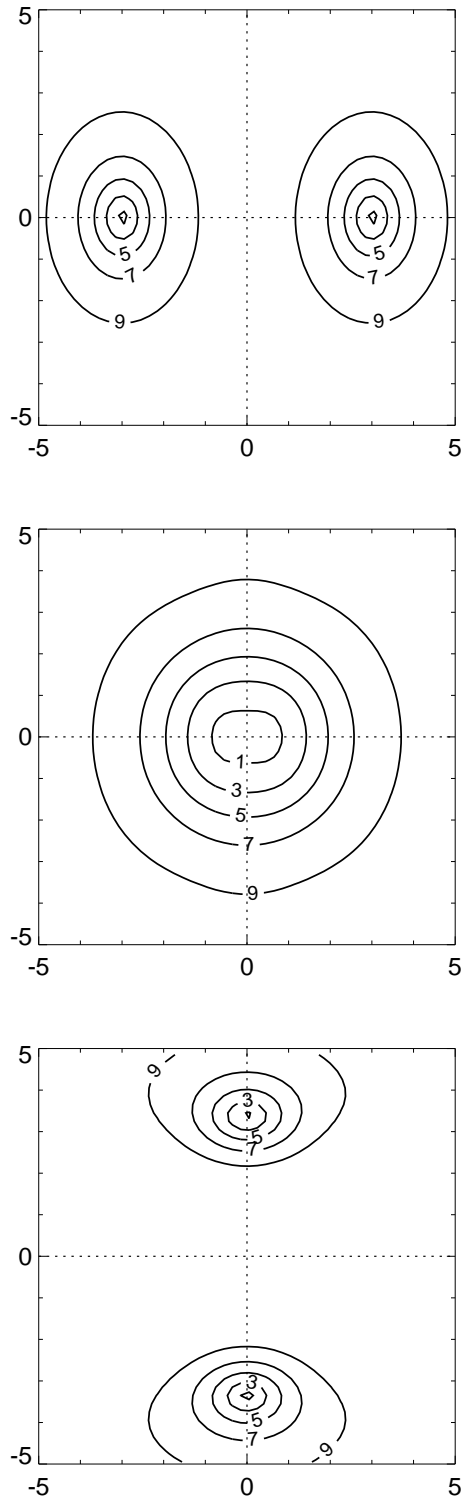


FIG. 7. Contour plot of the field  $10|\Omega|$  at three characteristic snapshots for the head-on collision simulation of vortices in an antiferromagnet. It is shown: the initial ansatz (upper entry, time  $t=0$ ), a snapshot at the time of collision (middle entry,  $t=4.2$ ), and well after collision (lower entry,  $t=8.4$ ). Contour levels as in Fig. 2.

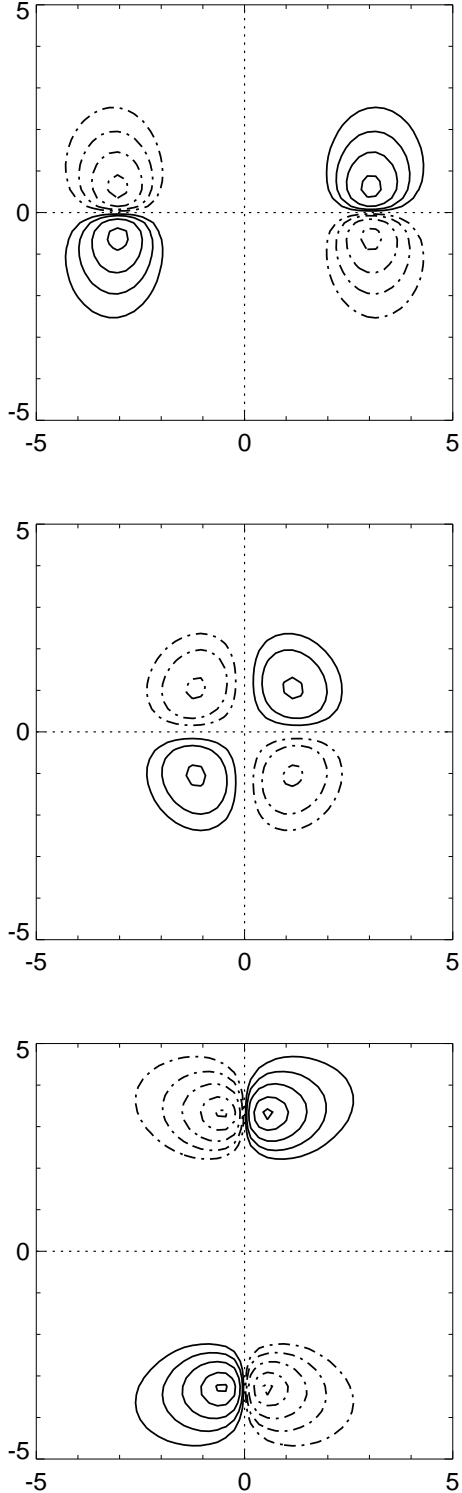


FIG. 8. Contour plot of the local vorticity  $\gamma$  of Eq. (13) for the vortices of Fig. 7. Contour levels as in Fig. 2.

The upper entry in the figure corresponds to the initial ansatz and each of the two vorticity dipoles should be compared to that given in the lower entry of Fig. 6. The two vortices in the first entry of Fig. 8 are approaching each other while their dynamical features, as described

by the vorticity, are not substantially modified. The repulsion which could decelerate them and make them turn round, is overcompensated by the large enough initial velocity. When the two vortices come close to each other (middle entry) the two pairs of vorticity lumps, lying in the upper and lower half plane, interact. The subsequent evolution of the vorticity lumps is governed by relation (8). In particular, this relation has to be applied to each of the vorticity lumps separately. As is indicated by the simulation, the lumps survive throughout the process and the simple dynamics implied by (8) is sustained during the scattering process. Following the discussion in Section II we examine the dynamics of lumps in a pairwise manner. The two pairs in the upper and lower plane tend to move along the  $y$ -axis. Consequently, the initial partners separate and two new vortices are formed which travel in opposite directions along the  $y$ -axis, as shown in the lower entry of the figure.

An equivalent approach is to follow the linear momentum of the solitons. The two pairs in the lower and upper half-plane have their linear momentums lying along the  $y$ -axis but with opposite signs. They subsequently tend to go off along the  $y$ -axis. The important numerical result is that the vorticity lumps roughly preserve their shape throughout the process. This is due to the fact that traveling vortices are stable solutions of the model.

We note here that our result is obtained when Eq. (8) is applied to each vorticity lump separately. We have been motivated to follow this approach because of its success with respect to studying the dynamics of vortex-antivortex pairs in a ferromagnet and because of the consistency of the picture with the linear momentum considerations. On the other hand a rigorous proof of its validity is lacking.

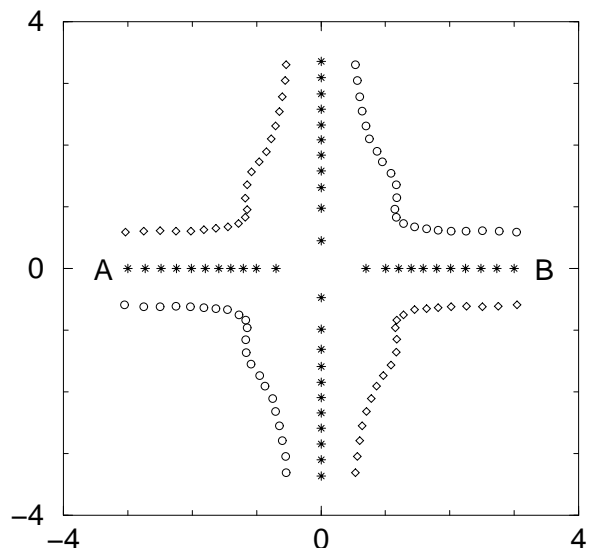


FIG. 9. Stars denote the zeros of  $\Omega$  during the numerical simulation of Fig. 7. We also trace the maximums (circles) and minimums (diamonds) of the vorticity. The vortices are initially located at points A and B. Symbols are plotted every 0.4 time units.



In Fig. 9 we track some characteristic points of the vortices throughout the simulation time. The stars denote successive points where the centers of the two vortices lie during the simulation, that is, where the complex function  $\Omega$  vanishes. The circles denote successive locations of the maximum and the diamonds the locations of the minimum of the vorticity distribution. We plot two circles and two diamonds at every time instant. At the beginning of the simulation the two vortices are centered at points  $A$  and  $B$  respectively. They immediately start to decelerate but when their centers reach a distance  $\approx 2.4$  they seem to accelerate considerably, they eventually merge at the origin and then they separate along the  $y$ -axis. The trajectories of the extrema of the vorticity show that after the collision it takes some time until the two new vortices are organized again. The velocity at the end of the numerical simulation is somewhat lower than that in the initial ansatz. This should be due to spin waves emitted during the process.

The remarks of the last paragraph on the motion of the vortex centers are in agreement with an analytical solution obtained in [25] representing scattering of solitons in an integrable chiral model. Close to collision time, the centers move according to the law  $x \approx \pm\sqrt{-t}$  ( $t < 0$ ). This gives a velocity  $dx/dt \rightarrow \infty$  as  $t \rightarrow 0$ . They collide at  $t = 0$  and the centers of the two new solitons, which emerge along the  $y$  axis, follow  $y \approx \pm\sqrt{t}$  ( $t > 0$ ).

The arguments presented in this section are certainly not sufficient to exclude, other than right angle, interesting possibilities of interaction and scattering of solitons. Nevertheless, they imply that the right angle scattering process is expected to be generic for solitons in two-dimensional Hamiltonian models. In the present work we have found no relation of the topology of the solitons to the right-angle scattering phenomenon, Therefore right-angle scattering is also expected to occur among non-topological solitons [26].

#### IV. CONCLUSIONS

We have given a description of the right angle phenomenon of solitons through numerical simulations, as well as arguments which suggest that it should be generic in two dimensions. Two systems have been examined. Vortex-antivortex pairs in planar ferromagnets and vortices in antiferromagnets. The peculiar scattering behaviour is mainly attributed to the fact that solitons are extended structures rather than point like particles. This point is accounted for by the representation of a traveling soliton through a pair of lumps. Furthermore, we find that these two lumps act as independent physical entities at the time of collision.

It is desirable to observe experimentally scattering of solitons in ferromagnetic and antiferromagnetic films. We expect that the present theoretical analysis will be useful in studies of systems of a lot of vortices [14] and in

particular in studies of the thermodynamics of magnetic systems. Suffice it to say that, in a magnetic material, vortices are expected to appear in pairs. In the study of the thermodynamics of layered antiferromagnets one expects to find the signature of topological excitations. The remark may prove important especially in view of the difficulty to observe isolated antiferromagnetic solitons due to the lack of a significant total net magnetization.

The right angle scattering pattern appears also and has been understood from the point of view of the geometry of the moduli space for BPS monopoles in a three-dimensional Yang-Mills-Higgs theory [27].

We have proceeded in the simulation of scattering of a vortex and an antivortex in the  $\sigma$ -model (2). We use an initial ansatz similar to that of Eq. (16). We simulate the time evolution of the system numerically and find that the vortices attract each other. They eventually collide at the origin and annihilate. It is quite interesting that the energy is dissipated at right angles. The phenomenon is presumably closely related to the present study. A similar simulation with corresponding results has been done in [28] for non-gauged cosmic strings.

The basic dynamical structure which leads to right angle scattering in Hamiltonian models is also present in the complex Ginzburg-Landau equation (CGLE) which describes nonlinear oscillatory media [29]. There is actually a variety of nonconservative systems where scattering behaviour analogous to that studied in the present paper has been observed. An interesting example is a 2D fluid layer subjected to externally imposed oscillations. Coherent structures are formed which are experimentally observed to scatter at an almost right angle [30].

#### V. ACKNOWLEDGMENTS

I am grateful to N. Papanicolaou and P.N. Spathis for providing me their numerical code which calculates the vortex-antivortex pairs used in the simulations of Section II and for useful discussions. I thank F.G. Mertens for discussion of the issues presented in this paper. I also thank L. Kramer for beneficial remarks on part of the text and L. Perivolaropoulos for his help with the numerical algorithm.

- 
- [1] A.P. Malozemoff and J.C. Slonczewski, *Magnetic domain walls in bubble materials* (Academic Press, New York, 1981)
  - [2] V.G. Bar'yakhtar, M.V. Chetkin, B.A. Ivanov and S.N. Gadetskii, *Dynamics of topological magnetic solitons-experiment and theory* (Springer-Verlag, Berlin, 1994)
  - [3] N. Papanicolaou and T.N. Tomaras, Nucl. Phys. B **360** (1981) 425;

- N. Papanicolaou in: R.E. Caflisch, G.C. Papanicolaou (Eds.) *Singularities in Fluids, Plasmas and Optics*, (Kluwer Academic Publishers, Amsterdam, 1993) pp. 151-158
- [4] N. Papanicolaou and P.N. Spathis, *Nonlinearity* **12** (1999) 285
- [5] B.I. Halperin, P.C. Hohenberg, *Phys. Rev.* **188** (1969) 898;  
F.D.M. Haldane, *Phys. Lett. A* **93** (1983) 464;  
S. Chakravarty, B.I. Halperin and D.R. Nelson, *Phys. Rev. B* **39** (1989) 2344
- [6] S. Komineas and N. Papanicolaou, *Nonlinearity* **11** (1998) 265
- [7] N.R. Cooper, *Phys. Rev. Lett.* **80** (1998) 4554
- [8] R.A. Leese, M. Peyrard and W.J. Zakrzewski, *Nonlinearity* **3** (1990) 773;  
W.J. Zakrzewski, *Nonlinearity* **4** (1991) 429;  
R.A. Leese, *Nucl. Phys. B* **344** (1990) 33
- [9] P.J. Ruback, *Nucl. Phys. B* **296** (1998) 669;  
R.S. Ward, *Phys. Lett. B* **158** (1985) 424;  
T. Ioannidou and W.J. Zakrzewski, *J. of Math. Phys.* (1998) **39** 2693;  
T. Ioannidou and W.J. Zakrzewski, *Phys. Lett. A* **242** (1998) 233
- [10] D.J. Gross, *Nucl. Phys. B* **132** (1978) 439
- [11] A.A. Thiele, *Phys. Rev. Lett.* **30** (1973) 230;  
A.A. Thiele, *J. Appl. Phys.* **45** (1974) 377
- [12] N. Papanicolaou and T.N. Tomaras, *Phys. Lett. A* **179** (1993) 33
- [13] N.S. Manton, *Ann. Phys.* **256** (1997) 114;  
N.S. Manton and S.M. Nasir, *Nonlinearity* **12** (1999) 851
- [14] F.G. Mertens, A.R. Bishop in *Nonlinear Science at the dawn of the 21st century* eds. P.L. Christiansen and M.P. Soerensen, Springer Lecture Notes (Springer, Berlin, 1999);  
A.R. Völkel, G.M. Wysin, F.G. Mertens, A.R. Bishop and H.J. Schnitzer, *Phys. Rev. B* **50** (1994) 12711
- [15] N. Papanicolaou and W.J. Zakrzewski, *Physica D* **80** (1995) 225
- [16] G. Stratopoulos and T.N. Tomaras, *Phys. Rev. B* **54** (1996) 12493
- [17] C.A. Jones and P.H. Roberts, *J. of Phys. A: Math. Gen.* **15** (1982) 2599
- [18] J. Staliunas *Chaos, Solitons & Fractals* **4** (1994) 1783
- [19] B. Piette, W.J. Zakrzewski *Physica D* **119** (1998) 314
- [20] H. Lamb *Hydrodynamics* (Sixth edition, Cambridge University Press, 1993),
- [21] J.S. Hesthaven, J.P. Lynov, A.H. Nielsen, J. Juul Rasmussen, M.R. Schmidt, E.G. Shapiro and S.K. Turitsyn, *Phys. Fluids* **7** (1995) 2220
- [22] P. Orlandi and G.J.F. van Heijst, *Fluid Dyn. Res.* **9** (1992) 179;  
H.J.F. van Heijst and J.B. Flór, *Nature (London)* **340** (1989) 212
- [23] S.V. Manakov, L.N. Shchur, *JETP Lett.* **37** (1983) 54;  
K.M. Khanin, *Physica D* **4** (1982) 261
- [24] A.A. Belavin, A.M. Polyakov, *JETP Lett.* **22** (1975) 245
- [25] R.S. Ward, *Phys. Lett A* **208** (1995) 203
- [26] M. Axenides, S. Komineas, L. Perivolaropoulos, M. Floratos, *Phys. Rev. D* **61** (2000) 085006;  
R. Battye and P. Sutcliffe, *Nucl. Phys.* **B590** (2000) 329
- [27] N.J. Hitchin, N.S. Manton and M.K. Murray, *Nonlinearity* **8** (1995) 661;  
M. Atiyah and N. Hitchin, *The geometry and dynamics of magnetic monopoles* (Princeton University Press, Princeton, 1988)
- [28] E.P.S. Shellard, *Nucl. Phys. B* **283** (1987) 624
- [29] S. Komineas, F. Heilmann, L. Kramer, *Phys. Rev. E* **63** (2001) 11103;  
I.S. Aranson, L. Kramer and A. Weber, *Phys. Rev. E* **47** (1993) 3231;
- [30] O. Lioubashevski, H. Arbell, and J. Fineberg, *Phys. Rev. Lett.* (1996) **76** 3959;  
J. Fineberg, O. Lioubashevski, *Physica A* **249** (1998) 10